Building Simulation

Seventh International IBPSA Conference
Rio de Janeiro, Brazil
August 13-15, 2001

A METHODOLOGY FOR MICRO-LEVEL BUILDING THERMAL ANALYSIS: COMBINING CFD AND EXPERIMENTAL SET-UPS

Ruchi Choudhary and Ali Malkawi, Ph.D.
The University of Michigan
Ann Arbor, MI-48105 - USA

ABSTRACT

Physical and computational simulations have been combined within a unique framework for the aim of establishing a methodology for micro-level building thermal analysis. Within this framework, each simulation mechanism overcomes the limitation of the other. The framework has been implemented by integrating an existing thermal chamber with Computational Fluid Dynamics (CFD) simulations. A detailed description of the procedure for affecting the combined methodology is the focus of this paper. In addition, the thermal chamber and the CFD prototype model of the chamber have been described. Finally, the application and scope of this work as a methodology for investigating indoor thermal conditions is discussed and future work is outlined.

INTRODUCTION

Airflow pattern determines the effectiveness of how a room is ventilated. It has a large influence on the thermal conditions within a space. Most building energy simulations model a space as a single node thereby assuming a fully mixed room with constant temperatures. While such an assumption is justified for determining overall system performance and energy loads of whole buildings, it does not allow for the analysis of local thermal behavior within a space. Particularly in cases where a more detailed information of the indoor climate is required, results obtained from a macro-level simulation represent a compromise. For the determination and prediction of detailed indoor climate that includes the airflow gradients and temperature fluctuations within a space, two prominent mechanisms exist – measurement and advanced airflow simulations (Loomans, 1998).

The study of localized thermal conditions within a building space essentially relied upon experimental studies, prior to the advent of powerful computational tools. Results from a good quality experiment have always been invaluable in being reliable and immediately applicable to actual conditions. However, experimental set-ups are generally cumbersome in time and cost. Being fixed in terms of location and spatial configuration, experimental measurements allow for specific cases to be studied under specific conditions. This not only imposes rigidity upon the investigation, but also prevents any generalized conclusions to be drawn from an experiment. Given the efforts and restrictions imposed by physical experiments, a computational environment offers an attractive alternative, where models can be constructed relatively quickly, and configurations or boundary conditions can be freely modified.

Of the various computational methods available, Computational Fluid Dynamics (CFD) has developed into the most powerful numerical technique for the investigation of indoor thermal conditions on a detailed level. Unlike most techniques, CFD fully resolves the Navier-Stokes equations upon the flow field and accounts for airflow property gradients even within a single space. However, due to the prevailing uncertainties in the modeling procedures and solver techniques, the reliability of quantitative information obtained from CFD remains difficult to determine – especially when heat transfer to the enclosure forms an important part of heat balance, (Chen et. al., 1998). For indoor thermal predictions, differences between measurements and computational simulations is almost always found (Loomans, 1998). To get a quantitative agreement the model has to be adjusted with measured data. Another challenge that has come forth through previous attempts at employing CFD based simulations is the representation of the thermal boundary conditions of the room surfaces. For a CFD simulation to be credible the set of boundary and initial conditions must be well posed.

Most attempts have been focused towards overcoming the deficiencies inherent in the two aforementioned mechanisms individually. With the vast improvement in discretization methods, numerical techniques and software systems, most of the building research industry has tended to shift towards powerful simulation modeling in lieu of physical experimentation, (Negrao, 1998; Gan, 1995). Conversely, attempts have been made to improve confidence in simulation environments like CFD by validating the simulation results with actual measurements, (Chen et. al., 1998; Tsou, 2001). An alternative would be to integrate the two

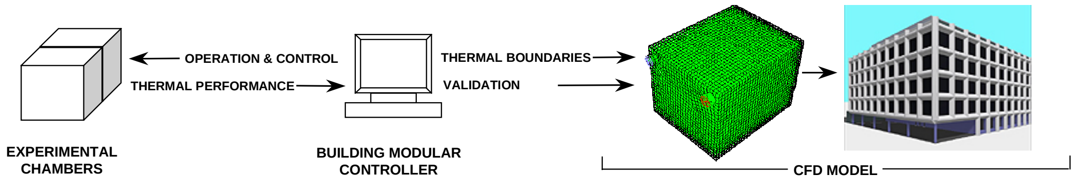

Figure 1. The Combined Methodology

simulation mechanisms within a single framework. Within such a framework, each of the simulation mechanisms can overcome the limitation of the other and result in a unique thermal prediction model that is both reliable and flexible.

THE METHODOLOGY

A methodology that combines the power of physical and computational simulations has been developed, (Figure 1). Within this framework the experimental chamber is set-up to mimic a unit or part of a system or configuration that needs to be modeled. An equivalent CFD model of the experimental chamber derives the necessary boundary inputs from the experimental set-up, thus ensuring the 'goodness' of the input data. The CFD-results are compared to measurements obtained from the experimental chamber, and the CFD model is adjusted in terms of mesh sizing, turbulence models, solver and discretization techniques till a good fit is obtained between the simulation results and measurements. Once stabilized and validated, the CFD model can be extended to represent the whole system or varied to test alternative spatial or/and system configurations.

The role of the physical and computational thermal chamber within the methodology is of a prototype, a working model of a unit within a building system. It has the potential to allow for partial components of a simulation to be validated, air-configuration systems to be controlled and operated, and feedback on the necessary boundary conditions to be elicited. The computational model of the experimental chamber also functions as a 'tester'. System configuration can be tested and stabilized as an isolated component before being extended to its actual configuration. The methodology promises (a) reliability by a continuous verification of CFD models in addition to specific determination of boundary and initial conditions required for the 'goodness' of the model, (b) flexibility by enabling a range of configurations and boundary conditions to be evaluated efficiently, and (c) economy, in such that multiple models, systems as well as numerical methods can be tested without having to construct a unique experiment for each case.

To initiate the process, an existing experimental chamber has been adapted to conform to the requirements of the methodology. This involved an accurate control over the experimental chamber and extensive data logging and monitoring capabilities. The chamber was modeled within the CFD environment developed by FLUENT (FLUENT 5.0.2, 1999). Boundary conditions at the room surfaces as well as at the supply inlet were determined from the measurements made within the chambers. Multiple preliminary simulations were conducted for achieving a stable numerical model and grid independency of the CFD output. CFD simulation results were compared to the measured data at 30 points within the room, under two sets of conditions: first, with an opaque façade, where the room was modeled for flow, energy and turbulence. Second, with a glazed façade that took into consideration heat transfer due to radiation. The result is a stabilized and validated CFD model that is capable of representing a perimeter zone, both with and without solar radiation.

EXPERIMENTAL CHAMBER

The experimental chamber is located in Ann Arbor, Michigan. The site is 42.17N, 871 meters above sea level. The south facade is unobstructed. The room is designed to provide flexibility for supply air diffuser location, amount and location of thermal mass, interior finish material as well as façade configuration.

The chamber is approximately the size of a one-person office, with dimensions of 8' x 8' x 8'. Only one wall of the chamber is exposed to the outside. The rest of the room surfaces are located inside a controlled laboratory. In effect, the chamber is constructed to model perimeter zones, but can be easily reconfigured to model an interior zone. Equipped with wheels, the chamber stands approximately 300mm above the ground, with free air circulating beneath it. This is to avoid modeling heat loss to the ground.

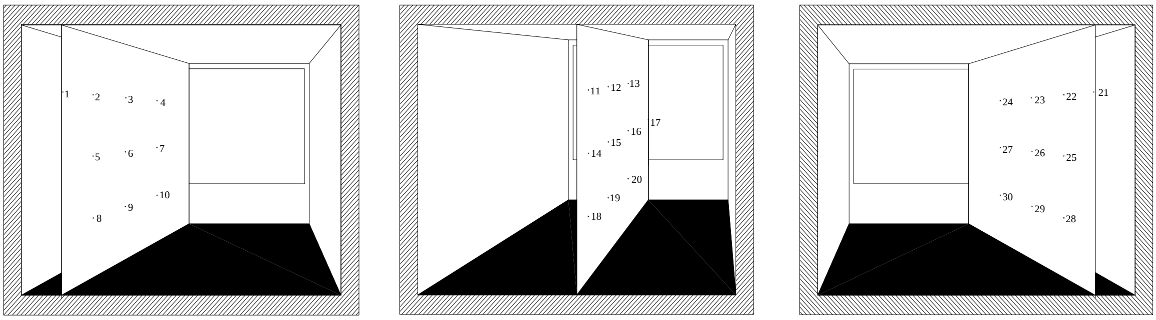

(a) East iso-Surface (b) Middle iso-Surface (c) West iso-Surface

<u>Figure 3. Location of the Temperature Sensors Shown from the North face of the Thermal Chamber</u>

The chamber envelope is constructed uniformly of 8" thick extruded Styrofoam sandwiched between layers of particleboard. The enclosure thus contains very Low Mass and has low thermal transmittance. The internal surfaces (walls, roof and floor) are highly insulated. Therefore, heat transfer to the interior domain is primarily through the south façade. The thermal properties of the materials have been tested and validated in previous experiments, (Leigh, 1991). The façade panels are mounted close to the external wall, above a knee wall, in order to eliminate shading effects. These panels are removable for installation of any type of façade components.

The experimental chamber provides a controlled environment for modeling thermodynamic processes such as heat transfer and comfort control. The test facility is designed to be very tightly sealed, in order to eliminate potentially uncertain air infiltration. If an experiment were to require it, air from the adjacent space can be drawn into the room at a carefully metered constant rate. Otherwise, the infiltration rate within the chambers may be assumed to be a minimal value of 0.15. The air volume supplied into the chamber is controlled through a speed controller connected to the fan motor.

Data is collected on the site of the test chambers by a centralized data acquisition system. The monitoring capabilities include two data loggers connected to microcomputers. One data logger is used for the measurements inside the chambers, and the second is used for the general weather data. A total of 20 copper-constantan thermocouples are installed to record 10 air-temperatures, 2 water temperatures, and 8 surface temperatures within the chamber. In addition to the thermocouples, 27 hoboes were mounted at pre-determined grid points within the chamber to measure local temperature profiles, (Figure 3). The airflow rate at the supply duct is also measured inside the chamber. The weather information is measured at the site and includes temperature, solar radiation, wind speed and humidity.

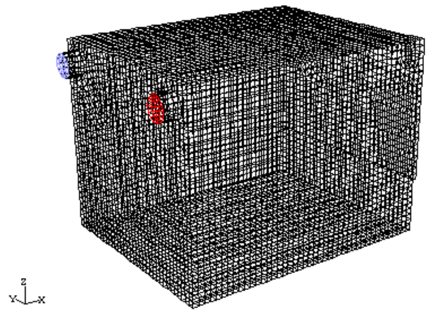

<u>Figure 4: The CFD Prototype</u>

<u>THE CFD PROTOTYPE</u>

A corresponding computational model of the experimental chamber was constructed within the CFD environment developed by FLUENT (FLUENT 5.0.2, 1999). It was meshed using a regular, structured grid with hexahedral mesh elements, (Figure 4). Multiple models with incrementing mesh density were prepared in order to check and establish grid independency of the results. Considering the airflow and heat transfer through the domain, three types of boundary are present - an inlet, an outlet and a series of solid walls. At the inlet, the pre-dominant flow direction was specified with the velocity component. The pressure-correction approach was set for solving the momentum equations in an uncoupled manner, using a prescribed provisional pressure distribution. The pressure field is later corrected by solving the Poisson equation that is developed from the continuity equation and the linearized momentum equations, (FLUENT 5.0.2, 1999).

This implies that the grid for computing pressure is staggered from the grid for the velocity components. The equations for turbulence, energy and radiation are solved thereafter, sequentially, using the previously updated values of other variables, (FLUENT 5.0.2, 1999). With this method, each dependent variable in a cell is computed implicitly, considering all the cells in the flow domain at the same time.

The flow within the chamber is turbulent considering the Reynolds number based on the inlet width and supply air velocity. The two-equation κ-ε turbulence model was set to model the flow, thus assuming a fully turbulent flow with the effects of molecular viscosity negligible. However, turbulent flows are significantly affected by the presence of walls where the no-slip condition has to be satisfied, (Shaw, 1992). Very close to the wall, viscous damping reduces the tangential velocity fluctuations, while kinematic blocking reduces the normal fluctuations (FLUENT 5.0.2, 1999). The standard turbulence model is primarily valid for turbulent core flows (i.e., the flow in the regions somewhat far from walls). To make the model conformable to wall-bounded domains, semi-empirical formulas called "wall functions" are used to bridge the viscosity-affected region between the wall and the fully turbulent region (FLUENT 5.0.2, 1999). Previous studies have shown that standard wall functions as used by FLUENT and most CFD programs do not produce an accurate representation of the heat transfer from internal room surfaces (Awbi, 1998; Costa et. al., 2000). The default distance of the point from the surface where the wall function is applied may not be suitable. However, standard wall functions seemed appropriate to initiate this model since heat transfer through the interior wall surfaces is negligible in the present case.

With the segregated solver, FLUENT automatically applies the first order upwind scheme to solve the convection terms in the equations. For the numerical diffusion terms, second order upwind scheme was applied to ensure accuracy of the solution. Hence, the boundary requirements, solver techniques, heat transfer, and turbulence conditions were set. In addition, the process of combining the physical chamber and its CFD model was initiated.

THE INTEGRATED PROCESS

The experimental chamber was controlled under constant supply air rate and supply temperature over a 13-day period. The total volume of 200cfm was supplied into the room through a 12” supply duct. The supply and return air ducts are of the same size and were located on the upper opposite, (east and west) corners of the north façade of the chamber. The temperature of the supplied air was held constant at 68 degF for the duration of the test period. At the end of the 13-day period, the data was analyzed to ensure appropriate control and validity of the measurements.

Data obtained from the experimental chamber was used to define the boundary conditions of the CFD model. Temperature measurements taken at the outer surface of the interior walls were used to specify fixed temperature boundary conditions at the exterior surface of the internal walls. As a result, FLUENT solves a one-dimensional conduction equation to compute the thermal resistance offered by the wall. Convection boundary condition was specified for the wall (south façade) exposed to ambient air, based upon the weather data measured on site. The heat transfer coefficient at the exterior (south facing) wall boundary was assumed to be constant over the surface and was approximated as a function of the measured wind speed. The Supply air at the inlet was controlled over the operation period, and was specified accordingly in terms of velocity, direction and temperature. At the outlet, the pressure was set to zero and the velocity, temperature and any turbulence variables have been computed based on the interior zone conditions.

Multiple CFD simulations were run to obtain both a stable and a converged solution. For model stability, solver techniques and discretization schemes were adjusted till a reasonable interior domain was realized. The simulation performed better with the Boussinesq model for density specification within the interior domain. In general, the Boussinesq specification is used for steady-state calculations when the changes in temperature are small. Convergence was checked with the following three criteria: (a) the residuals of the discretized conservation equations steadily decreased, (b) the variation of the flow variables at specified positions in the flow field were less than 1% over the last 100 time steps for absolute values larger than 0.01, (c) the values of the overall mass flow and heat transfer rate through the computational domain, (Loomans, 1998; FLUENT 5.0.2, 1999).

Once a stable and converged solution was obtained, CFD simulations of the experimental chamber were run by incrementing the grid density at every simulation. Results from the simulations, each with varying mesh density, were compared

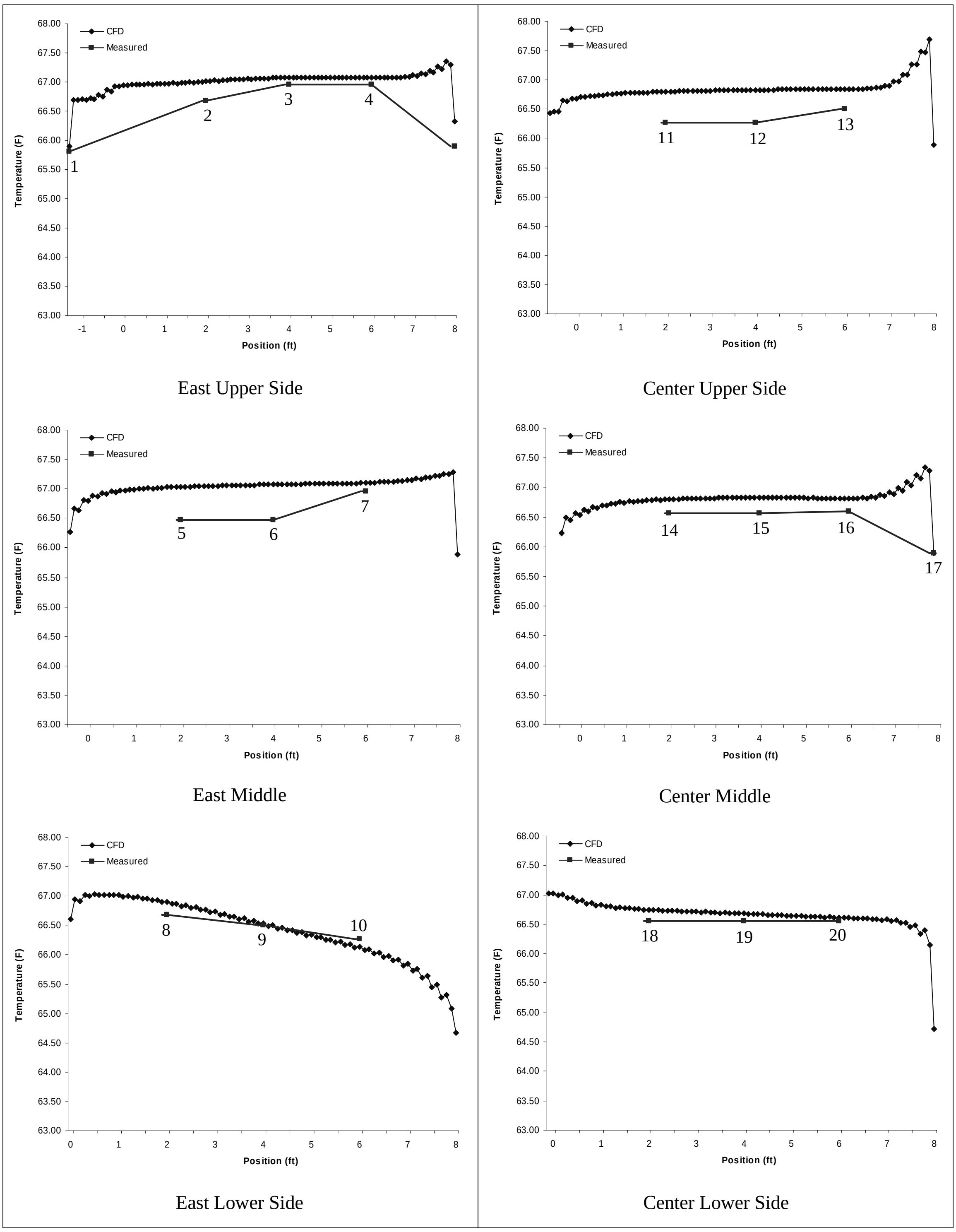

Figure 5a: Temperature Plots at the east iso-surface of the experimental chamber

Figure 5b: Temperature Plots at the middle iso-surface of the experimental chamber

Figure 5. A comparison of the temperature predictions from the CFD-output and temperature measurements at 30 points within the chamber. The sensor numbers listed on the data points of the measured results indicate their location, as given in Figure 4.

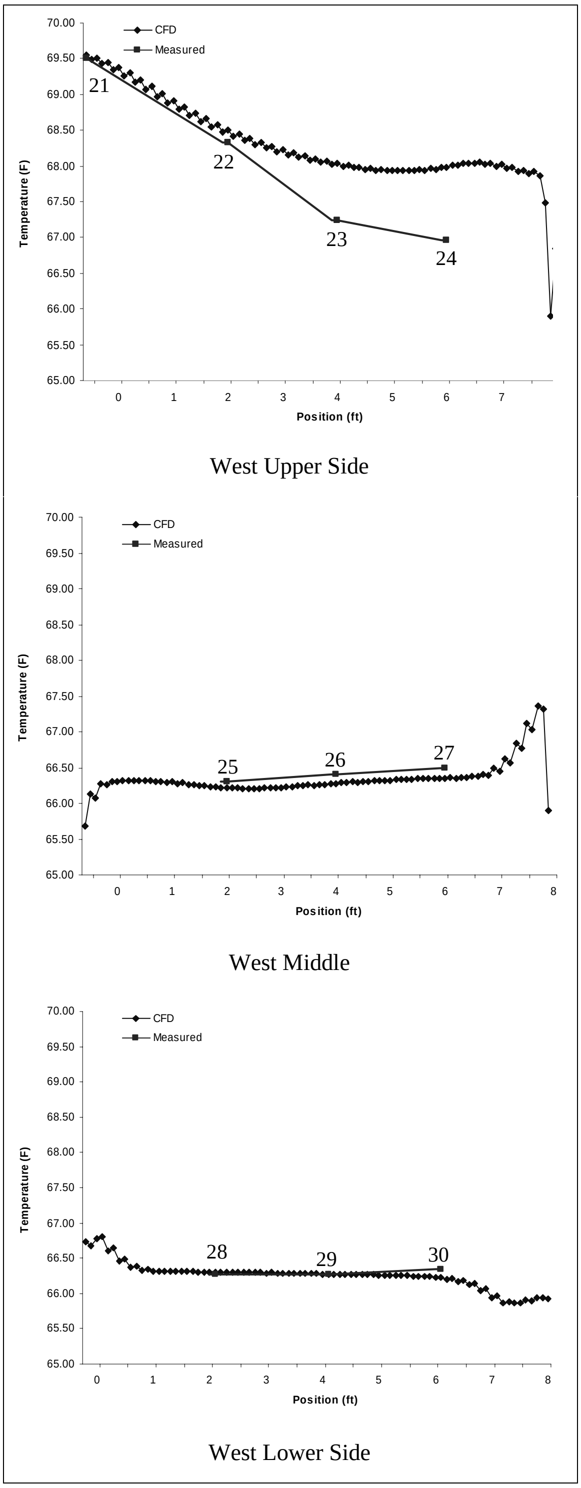

Figure 5c: Temperature Plots at the west iso-surface of the experimental chamber

till no difference was seen for at-least two subsequent mesh sizes. Finally, the gird spacing of 0.1875 was found to be most appropriate for the model. This implied computing the interior domain of the experimental chamber over 54588 nodes and 50341 cells. Grid independency for the solution of the CFD model was hence established.

To check for the reliability of the CFD results, temperature measurements at 30 points within the chamber – 28 interior air temperatures, and 2 surface temperatures – were compared to results obtained from the CFD simulation, (Figure 5). Temperatures at the upper region of the chamber were over-estimated, with the average difference of 0.4 DegF between the CFD results and the measurements. Overall, the simulation results showed a good agreement with the measurements in terms of temperature fluctuations within the room. On an average, the difference between the predicted and measured results at the 30 points is 0.2 DegF.

The airflow within the domain was pre-dominantly affected by the location of the supply inlet. Initialized from the east upper corner for the chamber, the supply air tended to 'stick' to the surface of the east wall before mixing into the interior domain, (Figure 6). This could be attributed to the airflow rate supplied into the chamber being more than what would be required for the given volume.

MODELLING RADIATION

With a stable and verified CFD model, the second stage of the experiment was initiated. The radiation model was added to a stabilized and calibrated model of the chamber. The advantage was that radiation, being a complicated phenomenon, could be isolated and analyzed individually. Moreover, by breaking the model in two stages, two experimental prototypes were obtained – one for modeling opaque perimeter or interior zones, and another for modeling perimeter zones with glazed facades.

The non-gray Discrete Ordinate (DO) model was used to model radiation. The spectral optical properties of the glazing were specified in terms of discrete wavelength intervals over which the properties of the glass remain constant. The spectral distribution as well as the properties of the double-glazed façade panel was acquired from the WINDOW 4.1 database, (LBL, 1994), compiled by the NFRC for analyzing window thermal performances. A diffuse fraction allows setting the portion of the radiation that is reflected specularly.

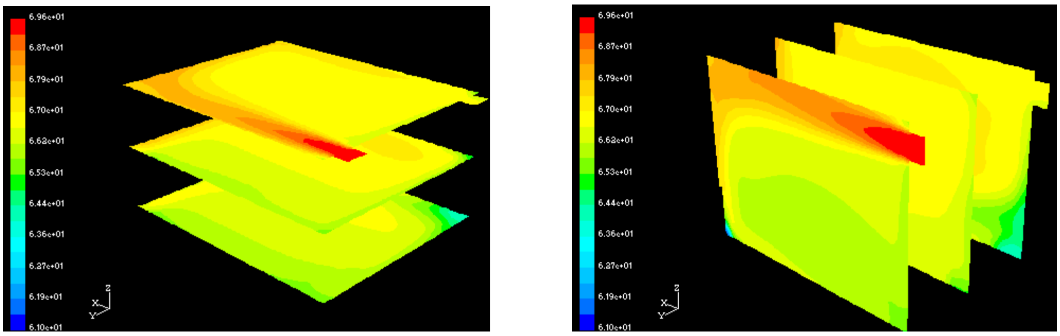

z iso-Surfaces of the Room Interior

y iso-Surfaces of the Room Interior

Figure 6. Contours of Temperature within the Chamber

Since the glass was clean, with a fine surface finish, the diffuse fraction of the irradiation was set to a value close to zero for each wavelength interval. The degree to which the interior wall surfaces reflect the incoming beam radiation was defined by setting the emissivity of the internal wall surfaces.

The façade panels of the experimental chamber were reinstalled with two 3' x 4' double glazed panels mounted on a knee-wall. The chamber was operated for another 13-day period under control conditions similar to those in the previous tests. That is, the temperature and flow rate at the supply was held constant – with 200cfm of air supplied at 78 DegF. As before, at the end of the 13-day period, data obtained from the experimental chambers was analyzed for its validity.

New values for the boundary conditions specified at the previous level were re-input to conform to the present measurements. These included the temperatures at the outer surfaces of the interior walls, heat transfer coefficient plus the outside air temperature at the external surface of the knee wall, and supply air specifications at the inlet.

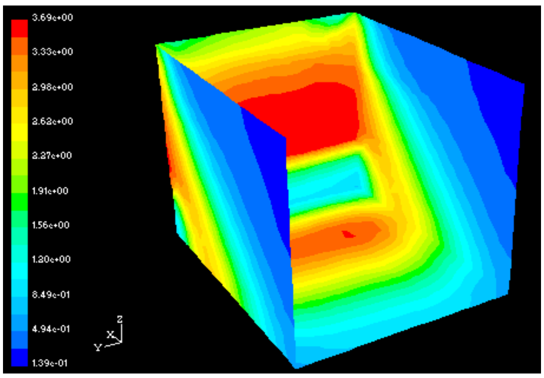

Figure 7: Incident Radiation Plotted for 3rd July at Noon

Additionally, Spectral Irradiation was specified in terms of an incident radiant heat flux (W/sq.mt) at each wavelength interval of the glazed surface. This was derived from the irradiation measured at the site of the experiment. The beam direction was specified to define the angle of the incoming radiation, as a unit vector. This was based on the sun position with respect to the receiving surface and was derived from solar calculations based on the time for which the simulation was run. The beam width is a property of the beam irradiating. These angles are $\Delta\theta$ and $\Delta\Phi$ and define a rectangular region on the spherical surface of the sky. For sunrays incident on a clean window, a very small beam width, say 1 deg and 1 deg in both directions were specified. The outer surface of the glass is also exposed to ambient air. Convection heat transfer boundary condition was hence applied, specifying the heat transfer coefficient and outside temperature.

The major difficulty posed by the current model was computational expense. To overcome the problem, the CFD model was simulated for two combinations of mesh density and angular discretization. The first simulation was run with a model of relatively coarse interior mesh but with angular discretization of 10x10 divisions. Conversely, the second simulation was run with a fine interior mesh, but with angular discretization of 6x6 divisions. The interior mesh spacing for both the above models was decided on the basis of the results obtained from the first stage. The results obtained from the above two simulations were also validated against temperature measurements taken within the experimental chamber. The simulation model performed better with the combination of a fine interior mesh and 6x6 divisions for the discretization of the sky, (Figure 7). An average difference of 0.3 DegF was reported between the CFD results and the measurements showing the temperature predictions for the radiation model.

CONCLUSIONS

The construction of an integrated methodology for modeling micro-level thermal simulations has been demonstrated. An existing thermal chamber has been successfully calibrated to its CFD prototype and validated results have been reported.

The CFD prototype of the thermal chambers promises the combined power of physical and computational simulations. This implies that by using the proposed methodology, reliability of results obtained from detailed thermal simulations can be highly increased. The notion of flexibility attributes to the many ways in which the computational model can be expanded without compromising the reliability of the simulation. The resulting integrated system allows the size and proportions of the CFD prototype to be varied, while the boundary conditions remain the same. In addition, the material of the enclosing surfaces can be changed and the configuration of the air-distribution can be modified. The system can also simulate different time and location by varying the parameters at the boundaries. All these changes can be made on a stable and validated computational model, thus increasing confidence in the results.

For unknown scenarios, the operating conditions within the experimental chambers can be easily controlled to obtain necessary boundary conditions and validation data. This eliminates the need to construct an experimental condition, each time a new HVAC system or operating mode to be tested. In addition, the integrated system allows different solution models within the CFD environment to be tested individually. This was effectively demonstrated when the radiation model was constructed on the basis of a stable opaque model of the CFD-prototype.

The most limiting factor of the combined methodology is the room geometry. Real-building scenarios often include complex geometries. The building geometry would have to be abstracted and simplified in order to model it with the CFD prototype. The applicability of the results to the actual building geometry needs to be tested. Another shortcoming of the model is that the validation of the results is based on temperature measurements. The thermal chamber needs to be enhanced by adding velocity and turbulence measurements. This is important because in many cases the flow gradients are the important indicators for assessing the validity of the CFD model.

ACKNOWLEDGEMENTS

We are grateful to Prof. Gretar Tryggvason at the Mechanical Engineering Department for his advice and support during the project.

REFERENCES

Awbi, Hazim B., “Calculation of Convective Heat Transfer Coefficients of Room Surfaces for Natural Convection”, Energy and Buildings 28 (1998) 219-227.

Chen, Q., Yuan, X., Hu, Y., Glicksman, L.R., and X. Yang, “Detailed Experimental Data of Room Airflow with Displacement Ventilation, Proceedings of Roomvent ’98”, vol. 1, pp133-140, Stockholm, 1998.

Costa, J.J., Oliveira, L.A., and D. Blay, “Turbulent Airflow in a Room With a Two-Jet Heating-Ventilation System-A Numerical Parametric Study”, Energy and Buildings 32 (2000) 327-343.

FLUENT Inc., “Fluent User’s Guide”, Fluent Inc., NH, USA, 1999.

Gan, Guohui, “Evaluation of Room Air Distribution systems Using Computational Fluid Dynamics”, Energy and Buildings 23 (1995) 83-93.

Leigh, Seung-Bok, “An Experimental Approach for Evaluating Control Strategies of Hydronic Radiant Floor Heating Systems”, Ph.D. Thesis, University of Michigan, Ann Arbor, MI, USA, 1991.

Loomans, M., “The Measurement and Simulation of Indoor Air Flow”, Ph.D. Thesis, Technische Universiteit, Eindhoven, 1998.

Negrão, Cezar O.R., “Integration of Computational Fluid Dynamics with Building Thermal and Mass Flow Simulation, Energy and Buildings 27 (1998) 155-165.

Shaw, C.T., “Using Computational Fluid Dynamics’’, Prentice Hall International Ltd, UK, 1992.

Tsou, Jin-Yeu, “Strategy on applying computational fluid dynamic for building performance evaluation”, Automation in Construction, Volume 10 (2001) 327-335.